ICAS-88-3.11.4

# EFFECTS OF MANEUVER DYNAMICS ON DRAG POLARS FOR AN AIRCRAFT WITH AUTOMATIC WING CAMBER CONTROL

John W. Hicks*
Bryan J. Moulton**
NASA Ames Research Center
Dryden Flight Research Facility
Edwards, California

## Abstract

The X-29A advanced technology demonstrator incorporates automatic cambering of the wing to enhance maneuverability and obtain the best aerodynamic performance. Trailing edge devices are deployed to improve performance as a function of flight condition and angle of attack. The flight control system of the X-29A aircraft was primarily designed to stabilize a highly statically unstable airframe. Within the control system, the automatic camber control loop was designed to provide the optimum lift-to-drag ratio for trimmed, stabilized flight. In the initial flight envelope expansion of this vehicle, the wing automatic camber control loop behaved in a markedly different manner during dynamic maneuvers than it did during the stabilized flight condition. This, in turn, affected the subsonic aerodynamic performance of the aircraft, which could be seen in the in-flight-measured aerodynamic drag polars and resulted in a higher drag level on the aircraft than in stable flight at the same angle of attack. The degree of increased drag levels was a direct function of maneuver rate.

This paper analyzes the effects of maneuver dynamics from the wing automatic camber control loop schedule on the aircraft flight drag polar results. Maneuver rate effects on the degree of increased drag will be shown. A discussion of the effect of changing the camber scheduling to better track the optimum automatic camber control lift-to-drag schedule will be given.

## Nomenclature

| | |
|---|---|
| ACC | automatic camber control |
| AR | analog reversion |
| c | wing chord |
| $C_D$ | coefficient of drag |
| $C_L$ | coefficient of lift |
| cg | center of gravity |
| D | aircraft drag |
| DR | digital reversion |
| $F_{ex}$ | excess thrust |
| $F_G$ | gross thrust |
| $F_N$ | net thrust available |
| $F_S$ | stick force |
| FCS | flight control system |
| FSW | forward-swept wing |
| GF1 | flaperon gain |
| GS1 | strake flap gain |
| h | altitude |
| KTRM | ACC canard trim gain |
| KSTR | ACC strake flap gain |
| L | aircraft lift |
| M | Mach number |
| MCC | manual camber control |
| $n_x$ | aircraft wind-axis longitudinal acceleration |
| $n_z$ | aircraft wind-axis normal acceleration |
| ND | normal digital |
| PA | power approach |
| PCM | pulse-code modulation |
| $\bar{q}$ | dynamic pressure |
| q | pitch rate |
| $\dot{q}$ | pitch acceleration |
| Re | Reynolds number |
| S | reference wing area |
| UA | up and away |
| W | aircraft gross weight |
| $\alpha$ | angle of attack |
| $\delta_c$ | canard surface position |
| $\delta_f$ | flaperon surface position |
| $\delta_s$ | strake flap surface position |
| $\theta$ | aircraft pitch attitude |
| $\phi$ | aircraft roll attitude |

*Aerospace Engineer.
**Aerospace engineering co-op student, Purdue University.

## Introduction

The flight test evaluation of new, advanced technology aircraft can have a direct effect on aircraft design and utilization of a specific technology. Flight testing can bring out a design deficiency in the aircraft that was not seen during the design and development stage. Often wind tunnel tests, other ground tests, predictive analysis techniques, and pilot-in-the-loop simulation likewise do not bring the deficiency to light until the flight phase of the actual vehicle. Past flight test techniques, which may have worked well on other aircraft, may prove to be inadequate in the precision flight testing of these new aircraft. An example of this will be highlighted later in this paper.

One of the recent trends in aircraft design is the use of automatic cambering of the wing to enhance maneuverability and obtain the best aerodynamic performance. These devices can be leading edge or trailing edge devices, or both, deployed over the flight envelope as a function of flight condition and angle of attack. The flight control system of the X-29A advanced technology demonstrator aircraft was primarily designed to stabilize a highly statically unstable airframe. The automatic camber control (ACC) loop of the control system was designed to optimize the lift-to-drag ratio for trimmed, stabilized flight. In the initial flight envelope expansion of this vehicle, the wing automatic camber control loop behaved in a markedly different manner during dynamic maneuvers than it did during the stabilized flight condition. Due to the built-in slow tracking rate of the control surface scheduling of this mode, the surface positions lagged well behind their optimum steady-state configuration as angle of attack changed. This, in turn, affected the aerodynamic performance of the aircraft, which could be seen in the subsonic in-flight-measured aerodynamic drag polars and resulted in a significantly higher subsonic drag level on the aircraft for a given Mach number than in stable flight at the same angle of attack. The degree of increased drag levels was a direct function of maneuver rate. The flight control system design approach was a conscious tradeoff between the desire for airframe stabilization and the recognized potential of aeroperformance loss during maneuvering flight. However, the degree of control surface ACC schedule-lag and the amount of drag penalty incurred was unexpected. It should also be pointed out that even with the adverse maneuver dynamic effects, the actual X-29A aeroperformance was still equal to or better than predictions subsonically and equal to predictions supersonically.

The X-29A was flown to evaluate seven integrated technologies for possible application in future generations of fighter aircraft. These technologies are the forward-swept wing (FSW) with graphite-composite skins; three-surface pitch control; highly relaxed aircraft static stability; digital fly-by-wire flight controls; a thin, supercritical airfoil; automatic wing cambering; and a close-coupled wing-canard configuration. The Defense Advanced Research Projects Agency (DARPA) began the project in 1977 with the Grumman Aircraft Systems Company (Bethpage, New York) as the aircraft designer and builder. The first flight of a 2-year flight envelope expansion phase was made in late 1984 at the NASA Ames-Dryden Flight Research Facility in California. Reference 1 summarizes the flight results of the envelope expansion phase. This flight phase was followed by a dedicated flight research phase to further exploit and evaluate the technologies. Ames-Dryden was the responsible test organization which was joined by Grumman and the U.S. Air Force Flight Test Center in the testing of the X-29A.

The aeroperformance flight research phase was flown to investigate the drag characteristics of the X-29A forward-swept wing. The predicted benefits of the FSW include increased wing aerodynamic efficiency and decreased induced drag levels up to 13 percent, compared to aft-swept-wing fighters. Another objective was to evaluate the benefits of the close-coupled wing-canard configuration. Dynamic flight test techniques were used to efficiently measure the drag polars as a function of angle of attack over the flight envelope Mach number.

This paper analyzes the effects of maneuver dynamics from the wing automatic camber control loop schedule on the aircraft flight drag polar results. Maneuver rate effects on the degree of increased drag will be shown. A discussion of the effect of changing the camber scheduling to better track the optimum automatic camber control lift-to-drag schedule will be given.

## Aircraft Description

### General Discussion

The X-29A (Fig. 1) is a single-seat, fighter-type aircraft incorporating several new technology concepts that synergistically work for aircraft performance improvements. The most notable feature is the FSW with a 29.3° leading edge sweep and a 5 percent thin supercritical airfoil section. The upper and lower surface wing skins are made of a graphite-epoxy composite material and are used to aeroelastically tailor the wing deflection and inhibit wing structural divergence. The wing has no leading edge devices, but incorporates full-span trailing edge, dual-hinged flaperons that are divided into three segments on each wing. The midwing and outboard segments are driven by a single hydraulic actuator, housed in a fairing under the wing. The inboard segment is driven by a separate actuator, located near the wing root. The two wing camber control modes are the automatic camber control (ACC), set by the flight control system as a function of flight condition, and the manual camber control (MCC), set in discrete 5° intervals by the pilot. In the ACC mode, the flaperons vary the camber of the wing to increase aerodynamic efficiency over the flight envelope. A schematic of the flaperon configuration can be seen in Fig. 2. The ACC mode also positions the canards and strake flaps along with the wing flaps to trim pitching moments and to give the best aerodynamic performance in steady-state flight. The MCC mode was used only as a flight test mode. Full flaperon travel was from 10° trailing edge up to 24.75° trailing edge down. Maximum flaperon rate was 68°/sec in response to pilot-commanded pitch inputs.

Another feature of the aircraft is its active three-surface pitch control configuration. In addition to the wing flaperons, this included the canards and the aft-mounted strake flaps. Symmetric deflection of these fully active surfaces is controlled by the flight control system to provide trim and pitch control. The canards are 20 percent of the wing area and act as a powerful lift and pitch generator. They are of an all-moveable single-piece construction with the leading edge traveling from 30° up to 60° down and moving at rates of up to 100°/sec. The strake flaps travel from 30° trailing edge up to 30° trailing edge down. The ACC schedule, which positions the surfaces for low drag, also attempts to keep the canard unloaded. Flaperons and strake flaps are positioned to force the canard to a reference position. Differential deflection of the flaperons provides the sole source of roll control. Yaw control is provided by a single-piece rudder mounted on a fixed vertical stabilizer.

The aircraft is powered by a single 16,000-lb-class F404-GE-400 afterburning engine. The engine is mounted in the fuselage with two side-mounted, fixed-geometry inlets that were optimized for transonic performance. Maximum aircraft takeoff gross weight is 17,800 lb with a 4000-lb fuel capacity in two fuselage and two strake tanks.

## Flight Control System and the ACC Mode

The flight control system (FCS) is a triply redundant digital/analog fly-by-wire system. Each of the three Honeywell (Minneapolis, Minnesota) HDP5301 dual-processor flight control computers contain both a digital and an analog backup computer operating in parallel. The high degree of airframe longitudinal instability (nominally 35 percent negative static margin subsonically) resulting from the presence of the canard on an otherwise neutrally stable wing-body necessitates high levels of stability augmentation. This is provided by the flight control system operating at an update rate of 40 Hz. The longitudinal control design is primarily a g-command system as a function of Mach number and altitude with feedback of normal load factor, pitch rate, and canard position. Fig. 3 presents a simplified block diagram of the longitudinal part of the primary digital mode of the X-29A.

The FCS consists of three flight modes: the prime normal digital mode (ND), the digital reversion mode (DR), and the analog reversion mode (AR). Each FCS mode has both an aircraft cruise mode, known as "up and away" (UA) and a power approach (PA) mode. Extensive gain scheduling is employed in each FCS mode. A more detailed description of this system can be found in Ref. 2.

The ACC loop of Fig. 3 is built around the canard position error signal. This error is computed as the difference between the actual position and the design schedule position, which is a function of Mach number, altitude, and angle of attack. This error signal is used to position the flaperons and strake flaps, which causes the canard to move to retrim the airplane. This process continues until the canard reaches its reference value. At that point all three surfaces are at their optimum performance positions. The optimum positions are based on wind tunnel data. Fig. 4 shows the design ACC flaperon schedule limit as a function of Mach number. Although the pilot can command high pitch rates with corresponding rapid control surface deflections for maneuvering flight, the maximum ACC flaperon tracking rate for steady-state flight is 2°/sec, which was sufficient for trimming in stabilized flight conditions and did not interfere with the short period control of the aircraft.

## Instrumentation System Description

The X-29A was instrumented with 691 parameters including measurements for structural loads, structural dynamics, flight controls, stability and control, aircraft subsystems, propulsion and performance, wing deflections, buffet, and external pressure distributions. All measured data parameters were telemetered to the ground for recording, real time analysis, and control room monitoring. The aircraft did not have an onboard recording capability. The 10-bit remote unit pulse-code modulation (PCM) system sampled data from 25 to 400 samples/sec, depending on the desired frequency range to be covered. A schematic of the instrumentation system can be seen in Fig. 5. The digital data were processed by five PCM units. The digital data and the output from the flight control computers ARINC 429 bus were merged by a digital interleaver. The data were downlinked as a serial PCM stream. A constant-bandwidth frequency modulation (FM) system was installed to process high-response acceleration and vibration data. This FM signal was merged with the rest of the digital data from the interleaver and downlinked along with the pilot's voice signals.

Aircraft instrumentation included a pitot-static noseboom with angle-of-attack and sideslip angle vanes, and two fuselage side-mounted pitot-static probes and angle-of-attack sensors. The instrumentation package used for the flight performance measurements were two body-mounted linear accelerometer packages and a rate gyro package for aircraft pitch, roll, and yaw attitudes, rates, and angular accelerations. One linear accelerometer set, termed the dynamic performance center-of-gravity (cg) package, had limited measurement ranges specifically tailored to the pushover-pullup maneuver described later in this paper. Its longitudinal and lateral accelerometer ranges were ±0.6 g and the normal accelerometer range was -1 to +3 g. The other accelerometer set, termed the center-of-gravity accelerometer package, had larger accelerometer ranges varying from ±1 g for the longitudinal and lateral accelerometers and -3 to +8 g for the normal accelerometer. Both packages were displaced from the actual aircraft center of gravity.

The F404-GE-400 engine had a full instrumentation set for monitoring engine operating characteristics, engine trim levels, and for calculating in-flight thrust. Measurements included inlet temperature, compressor and turbine speeds and pressures, combustor pressure, turbine exhaust temperature, and a 20-probe rake measurement of turbine exhaust pressure. Volumetric flow meters were used to measure main engine fuel flow, and afterburner pilot and main fuel flows. Special

augmentor static pressure instrumentation was installed as data input for a newly developed real-time in-flight net thrust algorithm, based on the Simplified Gross Thrust Method of the Computing Devices Company of Ottowa, Canada.[3] The flight engine was thrust-calibrated at the NASA Lewis Propulsion Systems Laboratory. In-flight net thrust accuracy of better than 2.5 percent was achieved. Details of the calibration results and thrust accuracy can be found in Ronald J. Ray's as yet unpublished NASA TP, "Evaluation of Various Thrust Calculation Techniques on an F404 Engine."

## Dynamic Maneuver Test Techniques Description

Dynamic flight test techniques are primarily used to quickly and accurately define the aircraft drag polar and lift curve characteristics at a constant Mach number over a range of angle of attack. This increases flight productivity and efficiency in determining the aircraft aeroperformance. Performance accelerometry measurement systems, such as the body-mounted accelerometer package of the X-29A, are used to measure aircraft accelerations along and normal to the flight path. These techniques have been used for years, particularly in the flight test of high performance fighter aircraft such as the F-4E, FB-111A, F-16, F-15, F-20, and the B-1 bomber.

The two dynamic maneuvers used on the X-29A were the pushover-pullup and the windup turn. Both maneuvers were preceded by 30-sec stabilized trim points for engine stabilization, as well as stabilization of aim Mach number and altitude. The pushover-pullup was used to define the drag polar and lift curves from the mid- to low-range of angle of attack. The maneuver test technique consisted of a pushover from the 1-g normal load factor at the wings-level stabilized flight condition to zero g normal load factor at a nominal g-onset rate of 0.2 g/sec. At the zero-g point, the aircraft was pulled up at the same g-onset rate to 2 g and returned to the 1-g level flight condition. Altitude and Mach number excursions were kept to a minimum. The windup turn maneuver was used to obtain the same data from the mid- to high-range of angle of attack, beginning from the angle of attack of the level, stabilized flight condition. Using the same g-onset rate as for the pushover-pullup maneuver, the windup turn was at a fixed power setting in which the aircraft descended, trading altitude for airspeed to hold a constant Mach number. As the maneuver progressed, the normal load factor and angle of attack increased to the aim conditions. For a given Mach number, the two maneuvers produced flight data that overlapped in coefficient of lift between 1 and 2 g, giving a full polar shape over the angle-of-attack range. This approach assures good data quality and test technique between the maneuvers. Fig. 6 shows a schematic drag polar representation of the angle-of-attack variation for a polar at a given Mach number. Detailed discussions of the X-29A flight test techniques can be found in Ref. 4.

For this particular study of maneuver dynamic effects, the windup turn and pushover-pullup g-onset rates were modified to increase the maneuver rate in a controlled fashion to examine the degree of loss of aeroperformance as a function of maneuver rate at a subsonic, a transonic, and a supersonic flight condition. Typical maneuver blocks consisted of slow, medium, and fast versions of the maneuver techniques previously described. Slow maneuvers took nominally 20 to 30 sec to complete while fast maneuvers lasted about 3 to 7 sec. G-onset rate varied from about 0.07 to 0.15 g/sec for "slow" maneuvers and about 0.50 to 0.715 g/sec for "fast" maneuvers. The fast maneuver rates represent typical modern-day high pitch rates required for fighter aircraft maneuvering. The control surface positions were tracked and compared against the predicted ACC schedule position for the given flight condition.

## Data Analysis Method

Aircraft coefficient of lift ($C_L$) and drag ($C_D$) were computed from the accelerometer method using the equations

$$F_{ex} = n_x W \tag{1}$$

then,

$$C_D = \frac{D}{qS} = \frac{F_N - F_{ex}}{qS} \tag{2}$$

$$C_L = \frac{L}{qS} = \frac{n_z W - F_G \sin \alpha}{qS} \tag{3}$$

The in-flight thrust calculation procedure is extensive and can be found in Ref. 5.

Using the accelerometer and rate gyro data inputs, angular rates and accelerations were used to correct the measured body-axis accelerations to the aircraft c.g. reference. Accelerometer data were transformed to the aircraft wind axis or flight path coordinate system by angular transformations through angles of attack and sideslip. Thrust corrections included estimated nozzle and spillage drag, as well as calculated ram drag corrections. A drag polar correction procedure had been developed prior to flight for the post-flight data reduction to adjust the data to the power-off, trimmed ACC schedule configuration, as used in generation of the wind tunnel data base. This is a standard flight test analysis technique that is used to correlate flight test results with wind tunnel predictions, but which did not work well on the X-29A aeroperformance data reduction. The procedure was only capable of providing trim drag corrections for deviations from the ACC trim schedule of up to 2° angle-of-attack and ±5° control surface deflections. These limits represent normal linear aerodynamic correction ranges. The large off-ACC schedule effects discussed in this paper could not be corrected by this procedure since the angle-of-attack and control surface deviations were too large.

## Results and Discussion

The primary objective of the FCS is to stabilize a highly unstable airframe. The ACC control loop was designed to position the surfaces so that the aircraft trimmed at the optimum lift-to-drag ratio during steady-state conditions, such as in wings-level stabilized flight or during a stabilized turn maneuver. As the angle of attack in-

creased during maneuvering flight, the flaperons would attempt to track to the ACC schedule at a 2°/sec slew rate over and above the control surface deflections for the commanded aircraft pitch rate, driving the canard error signal to zero, thus forcing the canards and strake flaps to their respective ACC positions for that flight condition. For sufficiently high $\alpha$, the flaperons would eventually saturate at the full down limiting position, as shown against Mach number in Fig. 4. In this full down condition, the canard and strake flap would then remain to trim and stabilize the aircraft beyond that angle-of-attack point. Thus in the nonsteady-state maneuvering condition typical of fighter aircraft, the aircraft would never have sufficient time to reconfigure the control surfaces to the optimum-performance ACC schedule and would always incur some off-design drag penalty.

During dynamic maneuvers, where angle of attack changes quickly, large deviations from the optimum ACC schedule for all three control surfaces can occur (Fig. 7). In the more extreme cases, the canards were as much as 13° off schedule, the strake flaps as much as 10° off, and the flaperons up to 20° off schedule. The amount of off-schedule deviation was found to be a strong function of maneuver rate, as the control surfaces attempted to trim the aircraft and follow the ACC schedule. Although considered a small overall contributor, some of the deviation is due to a slight difference between the actual angle of attack and the schedule trim angle of attack, as a function of time during the dynamic maneuver. Windup turns and pushover-pullups that were flown sufficiently slow (25 to 30 sec) allowed the surfaces to track the ACC schedule closely, such that little difference in performance could be measured. The same maneuvers flown at increasing rates resulted in greater deviations from the ACC schedule. Subsonic maneuver rate effects, comparing the ACC schedule to control surface positions for increasing rates, can be seen in Fig. 8. Given enough time, the control surfaces will eventually catch up and match the ACC schedule as the aircraft stabilizes.

As Fig. 4 shows, the largest downward flaperon travel range of 25° is in the subsonic speed regime. Once reaching supersonic conditions, the total flaperon deflection is limited to a maximum of 5° trailing edge down. This had a favorable effect on the amount of supersonic drag penalty incurred. Supersonically, the maximum flaperon deviation from the prescribed ACC schedule position was limited by the total allowable flaperon deflection range, no matter what the maneuver rate. This allowed the control surfaces subsonically to be further off the ACC schedule for a given dynamic condition than could occur transonically or supersonically. As a result, the drag penalty effect was seen to decrease or "wash out" as the aircraft speed increased through the transonic to supersonic flight condition. Maximum trailing-edge-up flaperon deflection remained at 10° over the vehicle Mach number range.

It should be emphasized that the X-29A drag polar results met or exceeded predictions even with maneuver dynamic effects and show a high performance potential compared to modern aft-swept-wing fighters. The maneuver dynamic impact on aeroperformance can be seen in Fig. 9. A subsonic, a transonic, and a supersonic polar band are shown for the range of maneuver rates from slow to fast windup turns and pushover-pullups. Drag levels were found to always increase with some change in lift as the control surfaces tracked further and further from the minimum induced-drag ACC schedule. Subsonically (Fig. 9(a)) the increased drag penalty was as much as 15 percent; decreasing transonically to 11 percent (Fig. 9(b)) for the same variable-maneuver rate range. This level of drag rise can result in a significant loss of aircraft instantaneous turning performance. As Fig. 9(c) shows, the supersonic drag levels were virtually insensitive to maneuver rate, giving the same drag level with no measurable penalty. An in-flight check of the wind tunnel-developed ACC schedule was made using the discrete MCC flaperon settings to fly the same drag polar maneuvers. Preliminary results indicate that the ACC schedule does appear to give an optimum lift-to-drag performance in its scheduling of the control surfaces.

These tests demonstrate the significance of maneuvering flight effects in the design of automatic cambering systems. Such systems that are designed to give the optimum aeroperformance control surface configuration as a function of flight condition, should be developed to track the schedule in the highly dynamic maneuvering environment of the fighter aircraft as well as in steady-state, stabilized flight. For the case of the X-29A, this could result in a performance increase of as much as 15 percent during dynamic maneuvering.

A gain in aerodynamic maneuvering performance through closer tracking of the ACC schedule on an unstable airframe may not be mutually compatible with the FCS performance. Increasing the ACC tracking rate on an inherently unstable airframe can be destabilizing and actually result in a loss of FCS performance. A limited analytical evaluation was made by the airplane contractor to increase the ACC schedule tracking rate for maneuvering flight by directly increasing the gain of the canard without adjusting the rest of the system gains for compensation. A fourfold increase in this gain was found to improve the ACC tracking, but resulted in unacceptable loss of FCS stability margins. Consequently, the airplane contractor proposed an alternative approach that is felt will improve the tracking rate without loss of FCS performance. However, this proposed improvement has yet to be evaluated.

## Concluding Remarks

The X-29A advanced technology demonstrator flight evaluation included the testing of a wing automatic camber control mode designed to stabilize a highly unstable airframe and to configure the control surfaces to provide an optimum lift-to-drag ratio for improved aerodynamic efficiency during stabilized flight. Subsequently, the performance flight research phase of the forward-swept wing revealed that the ACC control surface schedule adversely affected total aircraft drag during dynamic maneuvering flight. This was due to the slow tracking rate of this control loop. The three-surface pitch control configuration

lagged the ACC schedule as much as 20° for the flaperons, up to 13° for the canards, and up to 10° for the strake flaps during such maneuvers. This resulted in increased subsonic drag levels above the ACC-schedule flight results of as much as 15 percent which diminished to an 11 percent drag penalty transonically. There was no measurable drag penalty supersonically as the available range of control surface travel decreased with increasing airspeed above Mach 0.60. The degree of increased drag over that of the ACC configuration was found to be a strong function of the maneuver rate below Mach 1. Once stabilized in a maneuver, the control surfaces converged to the ACC schedule. Preliminary contractor analysis indicates the control surfaces can be made to follow the ACC schedule during dynamic maneuvering flight as well as in stabilized trimmed flight, but care must be taken since the increased control surface slew rate can be destabilizing to the airframe and result in a loss of flight control system stability margins.

## References


[1]Hicks, J.W., and Matheny, N.W., "Preliminary Flight Assessment of the X-29A Advanced Technology Demonstrator," AIAA-87-2949, Sep. 1987.

[2]Whitaker, A., and Chin, J., "X-29 Digital Flight Control System Design," AGARD-CP-384, Oct. 1984.

[3]Ray, R.J., Hicks, J.W., and Alexander, R.I., "Development of a Real-Time Aeroperformance Analysis Technique for the X-29A Advanced Technology Demonstrator," AIAA-88-2145, May 1988.

[4]Hicks, J.W., Cooper, J.M., Jr., and Sefic, W.J., "Flight Test Techniques for the X-29A Aircraft," NASA TM-88289, 1987.

[5]"F404-GE-400 In-Flight Thrust Program No. 83112," General Electric Co., Aug. 8, 1983.


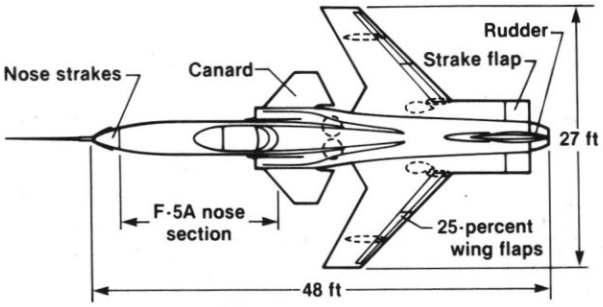


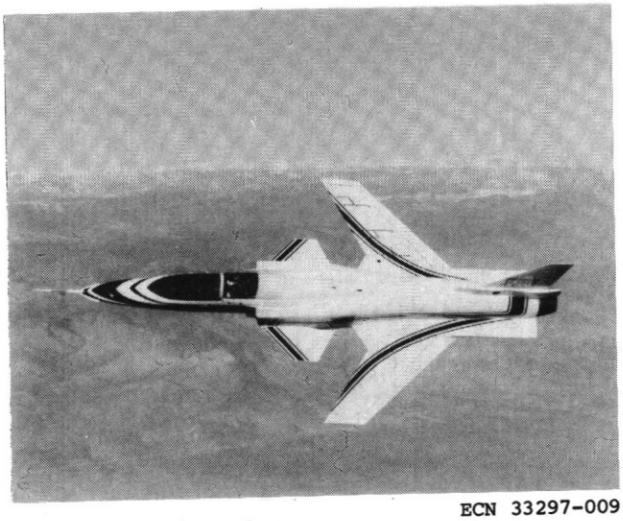


*Fig. 1 X-29A advanced technology demonstrator.*

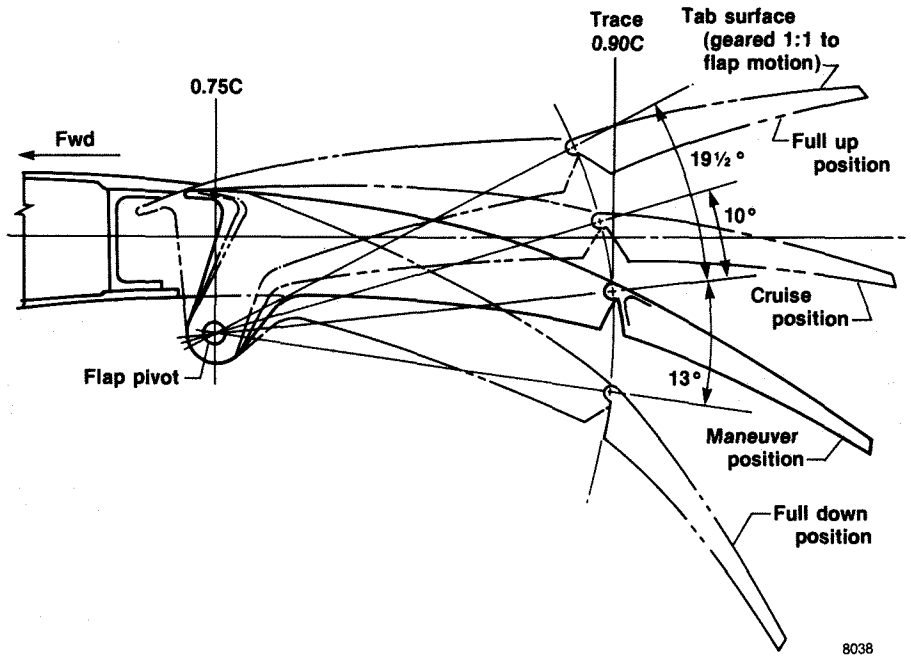


*Fig. 2 X-29A flaperon geometry (section normal to 0.75C).*

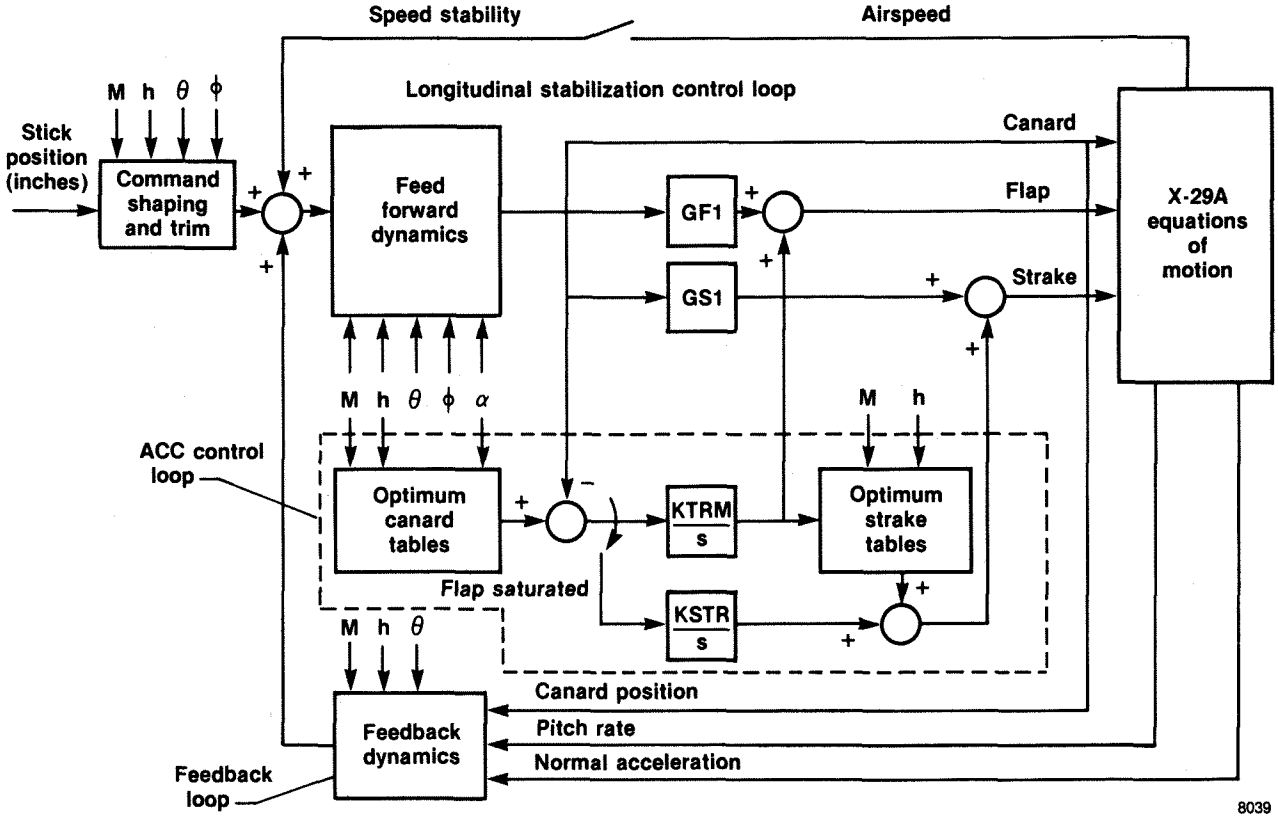


*Fig. 3 FCS longitudinal control system.*

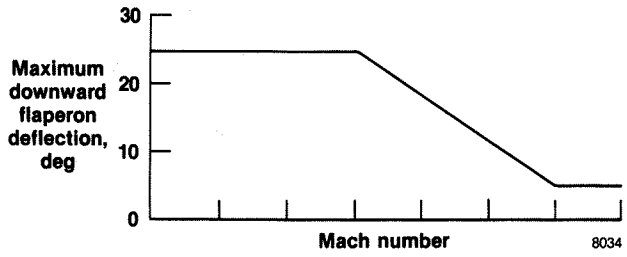


*Fig. 4 ACC flaperon limits in relation to Mach number.*

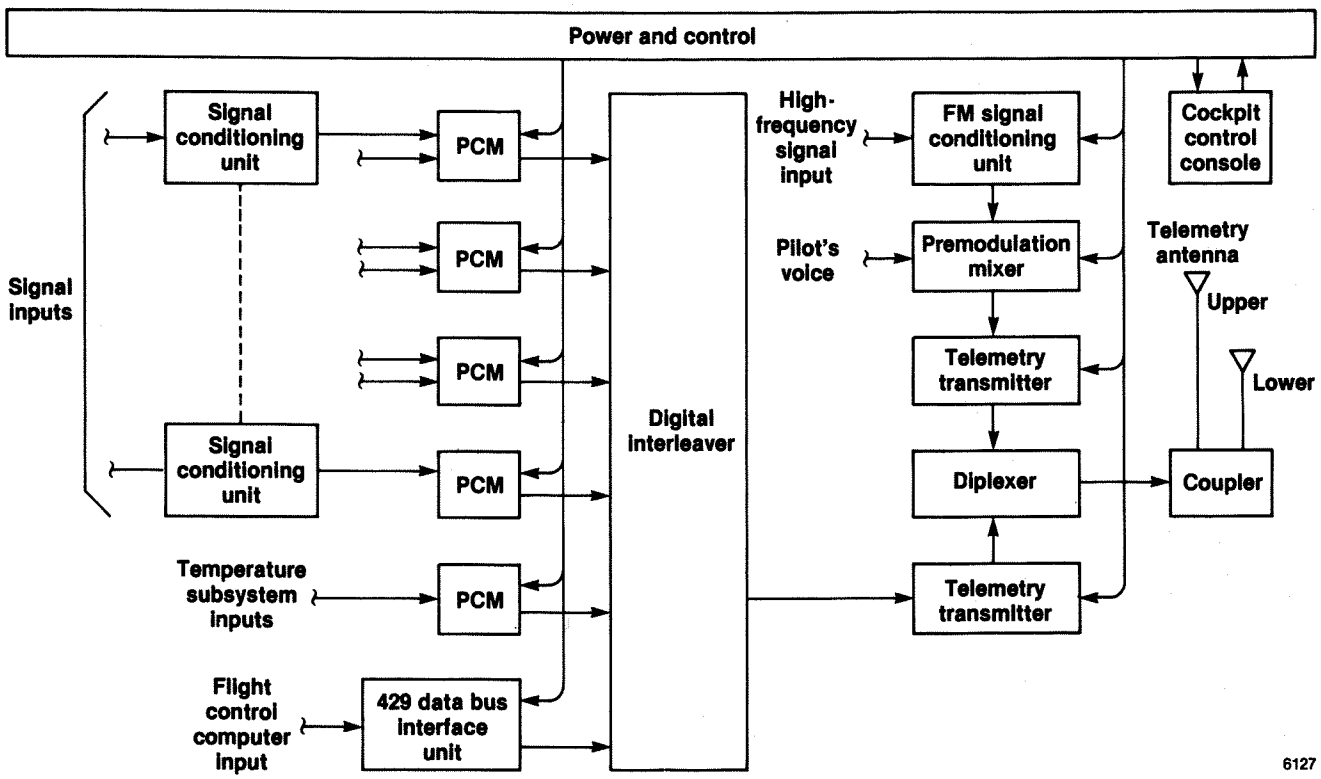


*Fig. 5 Aircraft instrumentation system.*

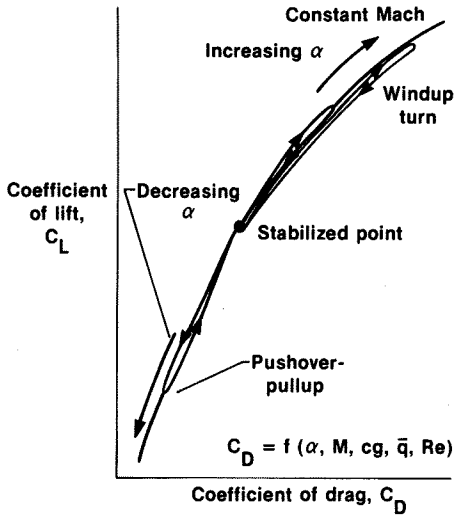


*Fig. 6 Dynamic maneuver drag polar generation.*

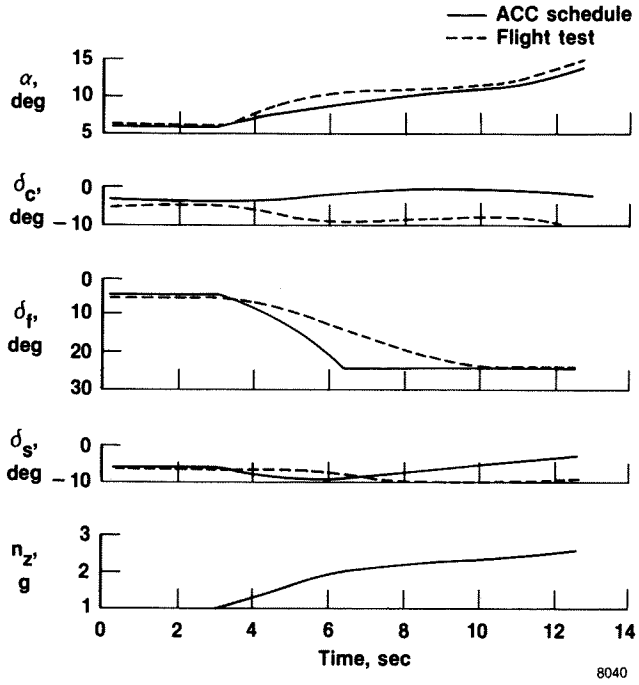


*Fig. 7 Off-ACC schedule effects during dynamic maneuvers.*

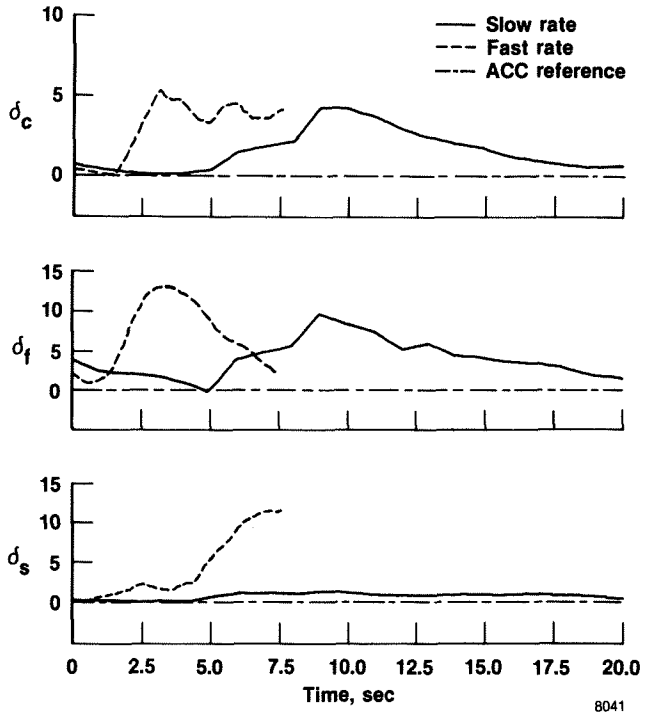


*Fig. 8 Control surface off-ACC reference increment during wind-up turn maneuvers.*

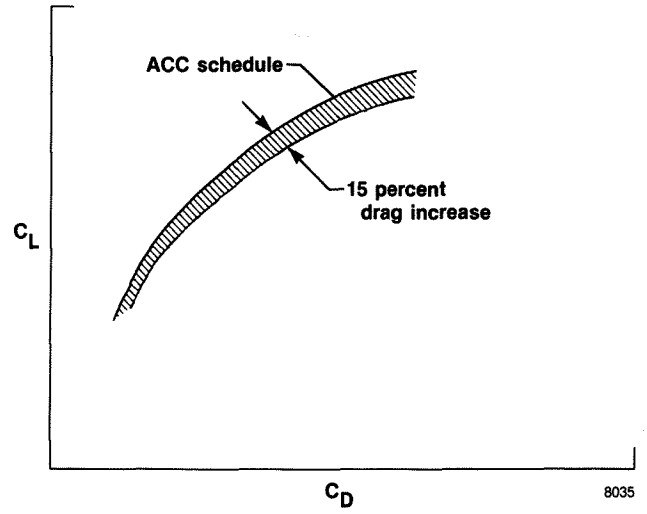


*(a) Subsonic case.*

*Fig. 9 Maneuver dynamics effects on aero-performance.*

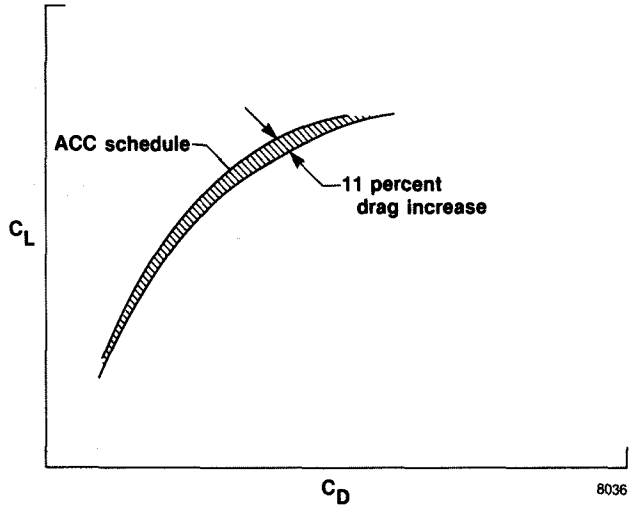


*(b) Transonic case.*

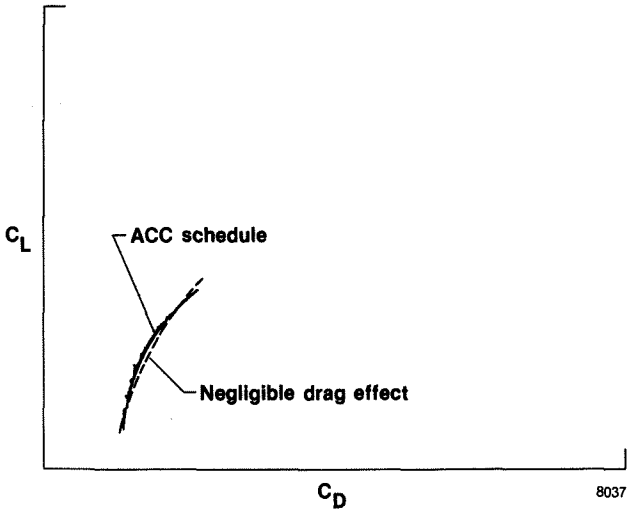


*(c) Supersonic case.*

*Fig. 9 Concluded.*